Colloid Polym Sci 280: 290–295 (2002)

SHORT COMMUNICATION

Tsuneo Okubo
Hisanori Ishiki
Hiroshi Kimura
Megumi Chiyoda
Kohji Yoshinaga

Kinetics analysis of colloidal crystallization of silica spheres modified with polymers on their surfaces in acetonitrile

Received: 6 June 2001
Accepted: 20 September 2001

T. Okubo (✉) · H. Ishiki · H. Kimura
Department of Applied Chemistry and Graduate School of Materials Science
Gifu University, Yanagido 1-1
Gifu 501-1193, Japan
e-mail: okubotsu@apchem.gifu-u.ac.jp
Fax: + 81-58-2932620

M. Chiyoda · K. Yoshinaga
Department of Materials Science
Kyusyu Institute of Technology
Kitakyusyu 804-0015, Japan

Abstract The nucleation and growth rates in the colloidal crystallization of silica spheres (136 nm in diameter) modified with polymers on their surface were measured by time-resolved reflection spectroscopy. The polymers were poly(maleic anhydride-*co*-styrene) [P(MA-ST)] and poly(methyl methacrylate) (PMMA). The induction period for nucleation decreased sharply when the sphere concentration increased. The crystal growth process consisted of a fast growing step leading to metastable crystals (rate v_1) and a slow growth rate accompanied by the formation of stable crystals. The crystal size of the P(MA-ST)/SiO_2 particles decreased from 0.4 to 0.06 mm, whereas v_1 increased from 13 to 37 μm/s, when the particle concentration increased. The slow step was also observed for almost all the samples but was not analyzed since the rate was too small. For PMMA/SiO_2 dispersions, the crystal size (0.17–0.3 mm) and v_1 (43–166 μm/s) did not show any relation to the particle concentration but showed a linear relationship with the molecular weight of PMMA. These results suggest the important role of the excluded-volume effects of the polymer layers around the silica surface. The contribution of the repulsion due to the electrical double layers is still effective in the colloidal crystallization in acetonitrile.

Keywords Crystals · Nucleation · Crystal growth · Reflection spectroscopy · Colloidal silica

Introduction

Many researchers clarified that colloidal crystals are mainly formed by Brownian movement of colloidal particles and also by the interparticle repulsion leading to the minimum dead space [1–17]. In other words, particles form crystal-like arrangements owing to the Brownian movement of the particles leading to maximum packing density.

When additional repulsive interactions, like excluded-volume effects by the electrical double layers and/or the layers adsorbed physically or attached chemically to the particles, exist colloidal crystallization takes place much more easily, even at very low sphere concentrations [1–9, 11, 13–17]. In previous articles we reported the kinetics of colloidal nucleation and crystallization in aqueous suspensions [18–26] and also in organic or aqueous organic solvents [27]; however, these reports discussed the excluded-volume effect from the electrical double layers only. Excluded-volume effects arising from the polymer layers were not studied in detail, especially at low particle concentrations.

In previous work, the rigidity of colloidal crystals of silica spheres coated with polymer layers were measured in acetonitrile and nitrobenzene in order to clarify the contribution of the excluded-volume effects from the polymer layers and the electrical double layers. In this work, colloidal nucleation and crystallization processes were studied for the same systems, i.e., silica spheres modified with poly(maleic anhydride-*co*-styrene) [P(MA-ST)]/SiO_2 and poly(methyl methacrylate) (PMMA)/SiO_2 in acetonitrile in order to clarify the

contribution of the excluded-volume effect from the polymer layers more in detail.

Experimental

Materials

Monodispersed colloidal silica spheres (136 nm in diameter) in ethanol, 23 wt% solid content, were kindly donated by Catalysts & Chemicals, Japan. To modify the silica spheres with P(MA-ST)/SiO_2, a colloidal silica dispersion (20 cm^3) was added to a mixture of 3.5 g P(MA-ST)–$Si(OMe)_3$ in 300 cm^3 1,2-dimethoxyethane and 20 cm^3 tetrahydrofuran [28]. The dispersion was stirred at 90 °C, and then 300 cm^3 solvent was removed by azeotropic distillation. Centrifugal separation from the suspension and drying under reduced pressure yielded the composite P(MA-ST)/SiO_2. IR (KBr): 2,950 (ν_{C-H}), 1,857 and 1,789 ($\nu_{C=O}$), 1,602 ($\nu_{C=C}$), and 1,130 (ν_{Si-O}) cm^{-1}. Silica spheres with PMMA/SiO_2 were prepared by the reaction of PMMA–$Si(OMe)_3$ with the colloidal silica in the same manner [28]. IR (KBr) for PMMA/SiO_2: 2,923 (ν_{C-H}), 1,753 ($\nu_{C=O}$), and 1,456 (δ_{C-H}) cm^{-1}. The IR spectra were recorded by a diffuse reflection method using a JEOL IR-5500 (Tokyo). The number-average molecular weight of the polymer (M_n) was determined by gel permeation chromatography, calibrated by a polystyrene standard, using tetrahydrofuran as an eluant. The amount of polymer (PA) on the surface of the silica spheres was determined by the mass decrease between 100 and 800 °C.

Acetonitrile and nitrobenzene were the purest grade reagents available commercially, were used without further purification, and were deionized with mixed beds of cation- and anion-exchange resins.

Reflection spectroscopy

Pyrex vials (2 ml in volume, 9-mm outside diameter, 35-mm high) with screw caps were used as observation cells. The cells were left to stand after inverted mixing. The nucleation and the crystallization started. These processes were followed by the growing Bragg reflection peaks after an induction time. The reflection spectra at an incident angle of 90° were recorded on a multichannel photodetector (MCPD-110B, Otsuka Electronics, Hirakata, Osaka prefecture) connected to a Y-type optical-fiber cable. The instrument was operated by a microcomputer (MC800, Otsuka Electronics).

Determination of the nucleation and crystal growth rates

Most kinetics measurements on colloidal crystallization showed an induction period after which the crystal growth starts, especially in diluted suspensions. This observation supports the fact that the kinetics of colloidal crystallization is explainable by the classical diffusive crystallization theory including nucleation and crystal growth processes [17, 19, 20, 29, 30].

The number of nuclei that germinated per unit time, i.e., the nucleation rate, v_n, is given by

$$v_n = N_n/t_i \ , \tag{1}$$

where N_n is the total number of nuclei which are formed during the nucleation process and t_i is the induction period. Here, we assume that the number of nuclei equals the number of single crystals formed. The number of sphere particles per mean size of a single crystal (N_c) is given for a cubic lattice by

$$N_c = \sqrt{2L^3/l^3} \ , \tag{2}$$

where L and l are the mean size of single crystals formed and the nearest-neighbor intersphere distance, respectively. The total number of colloidal spheres (N_T) in a unit volume is $\phi/[(4/3)\pi(d_0/2)^3]$. Then, v_n is given by

$$v_n = N_T/N_c t_i = \phi l^3 / \left[\left(4\sqrt{2}/3\right)\pi(d_0/2)^3 L^3 t_i\right] \ . \tag{3}$$

The size of the colloidal single crystals from the homogeneous nucleation, L, is estimated from the peak intensity of the reflection spectra [19]:

$$I \propto N_{cryst} L^3 \propto L^3 \ , \tag{4}$$

where N_{cryst} is the number of single crystals in the reflecting volume, which is directly proportional to the number concentration of crystals in the final stages of the crystallization process, being equal to the total number of nuclei formed in the whole course of crystallization. The final size of the crystals formed was determined independently using a charge-coupled-device (CCD) microscope (type VH-7000, Keyence, Osaka).

The first crystal growth rate of a metastable crystal, v_1, is given by [19]

$$v_1 = v_{1\infty}[1 - \exp(-s)] \ . \tag{5}$$

Here, σ is the relative supersaturation given by $(\phi - \phi_c)/\phi_c$. ϕ_c is the critical concentration of melting. $v_1\infty$ is the maximum crystal growth rate. Equation (5) is further simplified to

$$v_1 = v_{1\infty} - v_{1\infty}\phi_c/\phi \ . \tag{6}$$

Equation (6) means that the growth rate should decrease linearly as the reciprocal sphere concentration increases and was supported experimentally, but only at low particle concentrations [19].

Results and discussion

Reflection spectroscopy

Typical reflection spectra in the course of crystallization for P(MA–ST)/SiO_2 and PMMA/SiO_2 are shown in Figs. 1 and 2. The reflection peak sharpens with increasing crystallization, which corresponds to an increase in crystal size. The background intensity

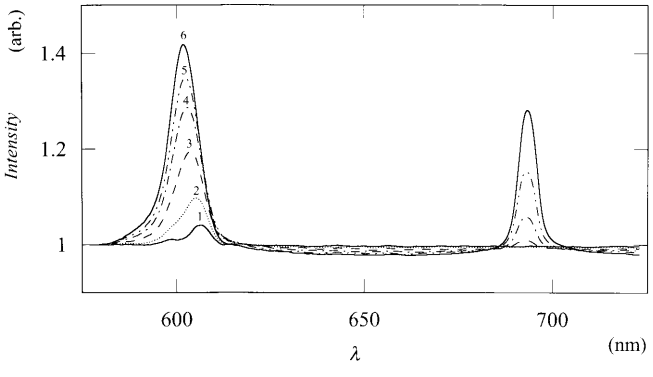

Fig. 1 Reflection spectra during crystallization of poly(maleic anhydride-*co*-styrene) [*P(MA-ST)*]/SiO_2 spheres in acetonitrile at 25 °C. $\phi = 0.0087$, $M_n = 6{,}500$, amount of polymer (*PA*) = 39.7 mg/g SiO_2. *1*: 0 s after stopped flow; *2*: 1.9 s; *3*: 4.0 s; *4*: 6.1 s; *5*: 7.9 s; *6*: 96.7 s

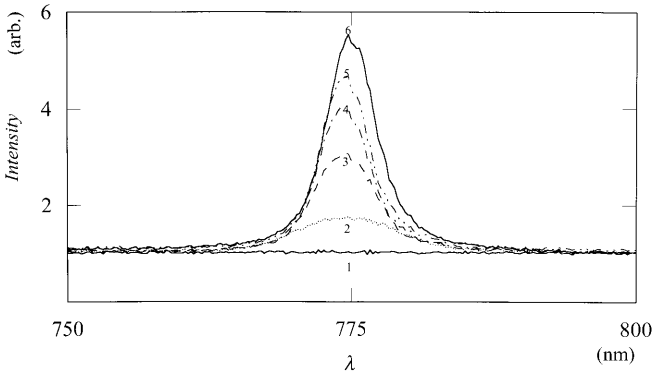

Fig. 2 Reflection spectra during crystallization of poly(methyl methacrylate) (*PMMA*)/SiO_2 spheres in acetonitrile at 25 °C. $\phi = 0.0442$, $M_n = 8{,}000$, PA = 17.8 mg/g SiO_2. *1*: 0 s after stopped flow; *2*: 2.0 s; *3*: 4.0 s; *4*: 6.0 s; *5*: 8.0 s; *6*: 24.9 s

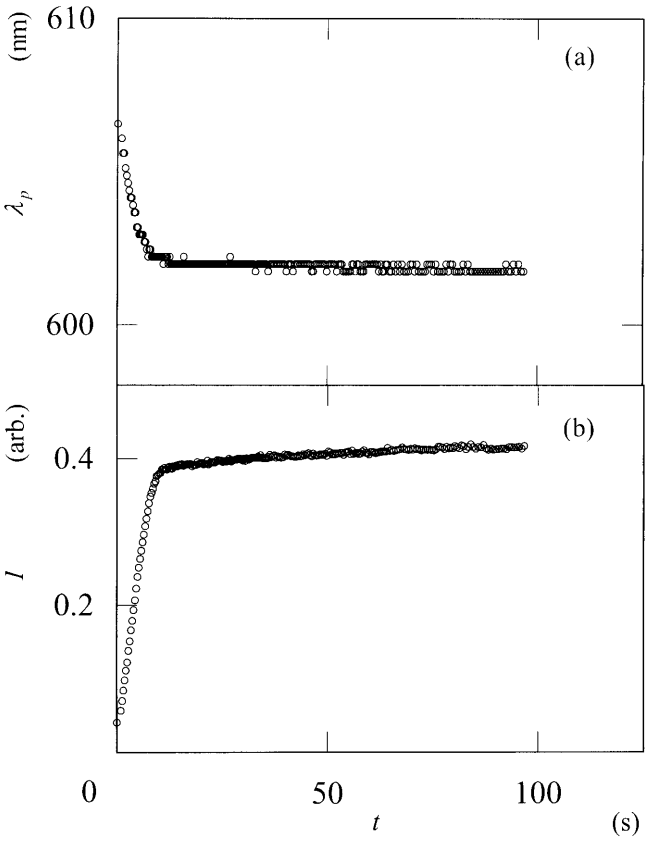

Fig. 3 Reflection peak wavelength during crystallization of **a** P(MA-ST)/SiO_2 and **b** PMMA/SiO_2 spheres in acetonitrile at 25 °C. **a** $\phi = 0.0087$, $M_n = 6{,}500$, PA = 39.7 mg/g SiO_2; **b** $\phi = 0.0442$, $M_n = 8{,}000$, PA = 17.8 mg/g SiO_2

decreased slightly during crystallization (Fig. 1), which is ascribed to the diminution in the multiple scattering of the dispersion. The structure of the colloidal crystals is, generally, face-centered cubic (fcc) (or, rarely close packed) or body-centered cubic (bcc). The fcc lattices are very stable and they transform to the bcc lattice at low particle concentrations, in the presence of salts, at elevated dispersion temperature, for spheres of high charge densities, and/or at high pressure [14]. Fcc and bcc lattices often coexist. Furthermore, the reflection spectrum of colloidal crystals shows a single peak, a double peak, or a single peak with a shoulder [31]. The two peak wavelengths were always close together, with a wavelength ratio of 1.027. The peak appearing at the longer wavelength is ascribed to the fcc lattice; the shorter wavelength to the bcc lattice.

The peaks around 600 nm (Fig. 1) are assigned to the (1,1,1) plane of the fcc lattice. The small peak at the shorter wavelengths around 598 nm in curve 1 is assigned to the (1,1,0) plane of the bcc lattice. Clearly, the peak from the fcc lattices increases faster during crystallization. The peaks at 693 nm cannot be assigned at present; however, these weak peaks appeared sometimes when a test-tube-type observation cell was used. It is highly plausible that the glass wall of the test tube in the spot area of the incident light is not completely smooth, and the reflection peak appeared from crystal planes other than the (1,1,1) plane, for example. The single peak in Fig. 2 for PMMA/SiO_2 does not allow assignment of the peak to a fcc or a bcc lattice.

The peak shifts during crystallization for the same samples as shown in Figs. 1 and 2 are shown in Figs. 3 and 4. Clearly, the peak wavelength, λ_p, decreased. This peak shift reflects the fact that metastable and loose crystals are formed in the first crystallization step before stable and compact crystals appear.

The nearest-neighbor intersphere distance, l, determined from the λ_p values observed at the final stage of crystallization using Eq. (7) are shown in Fig. 5.

$$l = 0.612\lambda_p/n \ , \tag{7}$$

where n is the refractive index of the suspension and was assumed to be that of acetonitrile. The values of the nearest-neighbor distance, l_0, on the other hand, are calculated by Eq. (8) [31].

$$l_0 = 0.904 d_0 \phi - 1/3 \ , \tag{8}$$

where d_0 is the diameter of the spheres, 136 nm in this work. The solid curve in Fig. 5 shows these l_0 values. Agreement between l and l_0 is satisfactory, though the former seems to be slightly smaller than the latter. This difference is mainly due to the fact that the particle concentration was calculated using the diameter of the parent silica spheres by neglecting the thickness of the polymer layers. The agreement demonstrates that the lattice spacing changes with the particle concentration. Furthermore, the crystals are formed by the Brownian movement of the spheres themselves and also by the

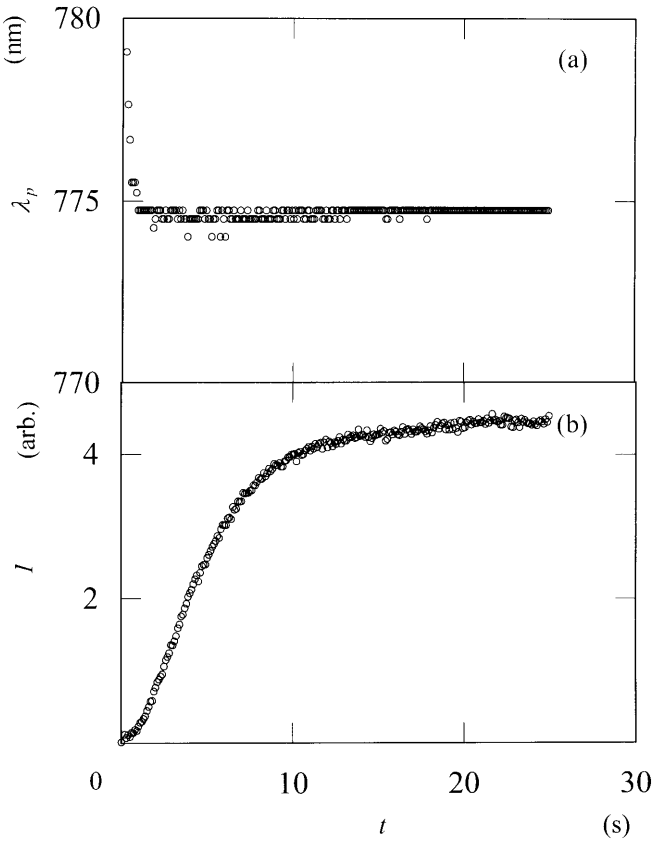

Fig. 4 Lattice spacing (l) of colloidal crystals of P(MA-ST)/SiO_2 (*circles*) and PMMA/SiO_2 (*crosses*) spheres in acetonitrile at 25 °C. The *solid curve* represents the calculation

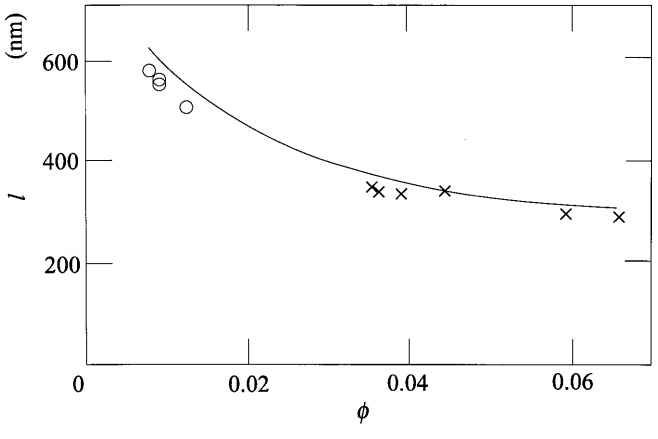

Fig. 5 Reflection peak intensity during crystallization of **a** P(MA-ST)/SiO2 and **b** PMMA/SiO_2 spheres in acetonitrile at 25 °C. **a** $\phi = 0.0087$, $M_n = 6{,}500$, PA = 39.7 mg/g SiO_2; **b** $\phi = 0.0442$, $M_n = 8{,}000$, PA = 17.8 mg/g SiO_2

excluded-volume effects from the electrostatic inter-sphere repulsive forces, or the polymer layers, or from both of them.

Nucleation process

The induction periods (t_i) were zero for almost all the experiments except those for P(MA-ST) at $\phi = 0.0078$ and PMMA at $\phi = 0.0442$, 1.5 and 0.25 s, respectively. These results show that the nucleation rates were too fast to be followed.

Previous studies [19, 20, 25] on the colloidal crystallization kinetics in aqueous media have clarified that v_n increased substantially as the particle concentration increased. v_n increased by 10^{10}-fold when ϕ increased 10^2-fold! Thus, the increase in the particle concentration is followed by an increase in v_n, then in the number of nuclei. This decreases the size of single crystals formed as discussed by Dhont et al. [32]. It should be mentioned that the size of the single crystals, both in aqueous and organic solvents, which is observed with the naked eye, is polydisperse as has often been observed [33, 34]. Therefore, the clear-cut separation of the nucleation step from the crystallization process is difficult, and the nucleation reaction may remain operative even during the crystal growth period.

Crystal growth process

Before calculation of the first growth rate, v_1, the apparent growth rate, k_1, was determined from the slope in the $I^{1/3}$ versus t plots. For this calculation, the final mean size of single crystals must be known. A CCD

Table 1 Properties of the colloidal crystals of poly(maleic anhydride-*co*-styrene) [*P(MA-ST)*]/SiO_2 and poly(methyl methacrylate) (*PMMA*)/SiO_2 spheres

Code	M_n	Amount of polymer (mg/g SiO_2)	ϕ	L (mm)	k_1 (1/s)	v_1 (μm/s)
P(MA-ST)/SiO_2						
01	6,500	39.7	0.0078	0.39_1	0.032	13
01	6,500	39.7	0.0078	0.43_5	0.048	21
02	6,500	39.7	0.0087	0.12_5	0.17_9	22
02	6,500	39.7	0.0087	0.12_5	0.15_1	19
02	6,500	39.7	0.0087	0.13_5	0.17_0	23
03	6,500	39.7	0.0122	0.057	0.33_7	19
03	6,500	39.7	0.0122	0.057	0.44_7	25
03	6,500	39.7	0.0122	0.066	0.56_6	37
PMMA/SiO_2						
01	8,000	17.8	0.0442	0.27_5	0.28_9	79
01	8,000	17.8	0.0442	0.26_3	0.32_1	84
02	10,000	37.0	0.0390	0.20_4	0.21_2	43
02	10,000	37.0	0.0390	0.28_5	0.25_1	72
03	10,000	55.0	0.0357	0.29_6	0.46_1	136
04	10,800	40.5	0.0594	0.22_3	0.21_8	49
04	10,800	40.5	0.0594	0.3	0.28_2	85
05	15,000	16.0	0.0353	0.20_8	0.66_7	139
05	15,000	16.0	0.0353	0.21_9	0.75_8	166
06	15,000	68.7	0.0659	0.17	0.77_5	132

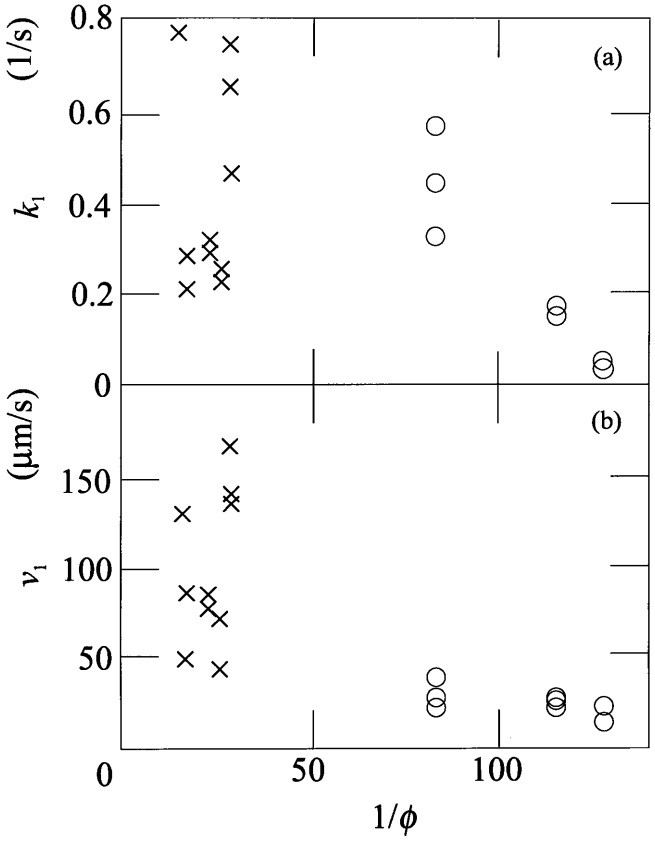

Fig. 6 Growth rate coefficient, k_1, and **b** growth rate, v_1, of P(MA-ST)/SiO_2 (*circles*) and PMMA/SiO_2 (*crosses*) spheres in acetonitrile as a function of sphere concentration at 25 °C

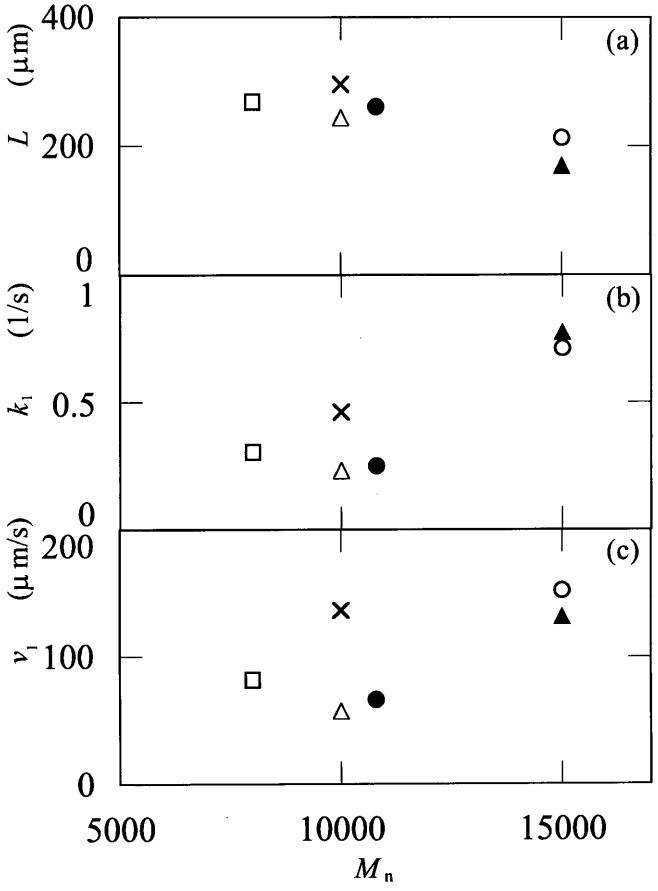

Fig. 7 Crystal size, **b** k_1 and **c** v_1 in acetonitrile as a function of molecular weight of PMMA at 25 °C. *Open circles*: PA = 16.0 mg/g SiO_2, $\phi = 0.0353$; *crosses*: 55.0, 0.0358; *open triangles*: 37.0, 0.0390; *squares*: 17.8, 0.0442; *filled circles*: 40.5, 0.0594; *filled triangles*: 68.7, 0.065

camera and close-up photography were used to measure the size, L. The results for P(MA-ST)/SiO_2 and PMMA/SiO_2 are shown in Table 1. L for P(MA-ST)/SiO_2 decreased sharply when the particle concentration increased, especially at low concentrations. This dependency of L with ϕ was often observed [11, 14, 15, 34, 35]. The L values for PMMA/SiO_2 spheres were quite insensitive of the particle concentration. The reason is that the polymers differ in the M_n and PA.

k_1 and v_1 thus estimated for P(MA-ST)/SiO_2 and PMMA/SiO_2 as a function of the reciprocal particle concentration are shown in Fig. 6. The linearity between v_1 and $1/\phi$ (see Eq. 6) was satisfactory for P(MA-ST)/SiO_2, The maximum growth rate, v_∞, was about 50 μm/s.

We assume that Eq. (5) is applicable and that the maximum growth rate is determined by the diffusion of single spheres near the crystal face. Then, Eq. (9) holds:

$$v_\infty = 4D_0/\xi \ . \tag{9}$$

Here ξ is the mean diffusion length (path) and D_0 is the diffusion coefficient of spheres in the crystallization suspension. When ξ is assumed to be the mean intersphere distance minus the sphere diameter, l–d_0 ($l = 0.57$ μm at $\phi = 0.01$ in this work), and D_0 is the diffusion coefficient of spheres in the gaslike state calculated by the Stokes–Einstein equation, v_∞ is given by

$$v_\infty = 4k_B T/3\pi\eta d_0(l - d_0) \ , \tag{10}$$

where d_0 is the sphere diameter. Calculation of v_∞ leads to 80 μm/s, which is not far from the observed value of 50 μm/s. The experimental errors of the v_1 values of PMMA/SiO_2 were large, as is clear in Fig. 6. This is clearly due to the fact that the polymers having M_n and PA values differing from each other have been compared.

It should be noted here that the v_1 values for the PMMA/SiO_2 spheres were in the range 50–150 μm/s, so several values are larger than the calculated values (80 μm/s). D_0 should be the diffusion coefficient in the supersaturated liquids. Furthermore, the mean diffusion length (ξ) is clearly overestimated when $\xi \cong l$–d_0 is taken, since the colloidal spheres in supersaturated liquids must

move in a cooperative manner as a consequence of the electrostatic repulsive forces. In this sense, the colloidal crystals are quite similar to fused metals. Slight movement of the effectively enlarged spheres including the excluded volume of the adsorbed layers and the electrical double layers will be enough to allow crystallization. Thus, the slight disagreement between the calculation and the observation is explained by the uncertainties of D_0 and ξ.

The v_1 values of $PMMA/SiO_2$ increased linearly with the molecular weight of the polymer (Fig. 7). This demonstrates clearly that an increase in the thickness of the adsorbed layers increases the crystallization rate. Furthermore, the excluded-volume effect from the adsorbed layers of the polymers plays an important role for the crystallization, though the role of the electrical double layers is still important in the crystallization process.

Acknowledgements M. Komatsu and M. Hirai of Catalysts & Chemicals Ind. Co. (Tokyo and Kitakyusyu) are greatly thanked for providing the silica samples. Akira Tsuchida of Gifu University is acknowledged for his valuable comments. The Ministry of Education, Science, Sports and Culture is thanked for Grants-in-Aid for Scientific Research on Priority Area (A) (11167241) and for Scientific Research (B) (11450367). T.O. greatly thanks the late Professor Emeritus Sei Hachisu for his continual encouragement and comments on our work on colloidal crystals.

References

1. Vanderhoff W, van de Hul HJ, Tausk RJM, Overbeek JTG (1970) In: Goldfinger G (ed) Clean surfaces: their preparation and characterization for interfacial studies. Dekker, New York, pp 15–44
2. Hiltner PA, Papir YS, Krieger IM (1971) J Phys Chem 75:1881
3. Kose A, Ozaki M, Takano K, Kobayashi Y, Hachisu S (1973) J Colloid Interface Sci 44:330
4. Williams R, Crandall RS, Wojtowicz PJ (1976) Phys Rev Lett 37:348
5. Mitaku S, Ohtsuki T, Enari K, Kishimoto A, Okano K (1978) Jpn J Appl Phys 17:305
6. Lindsay HM, Chaikin PM (1982) J Chem Phys 76:3774
7. Pieranski P (1983) Contemp Phys 24:25
8. Ottewill RH (1985) Ber Bunsenges Phys Chem 89:517
9. Aastuen DJW, Clark NA, Cotter LK, Ackerson BJ (1986) Phys Rev Lett 57:1733
10. Pusey PN, van Megen W (1986) Nature 320:340
11. Okubo T (1988) Acc Chem Res 21:281
12. Russel WB, Saville DA, Schowalter WR (1989) Colloidal dispersions. Cambridge University Press, Cambridge
13. Stevens MJ, Falk ML, Robins MO (1996) J Chem Phys 104:5209
14. Okubo T (1993) Prog Polym Sci 18:481
15. Okubo T (1994) In: Schmitz KS (ed) Macro-ion characterization. From dilute solutions to complex fluids. ACS symposium series 548. American Chemical Society, Washington, DC, pp 364–380
16. Okubo T (1997) Curr Top Colloid Interface Sci 1:169
17. Okubo T (2001) In: Hubbard A (ed) Encyclopedia of surface and colloid science. American Chemical Society, Washington, DC, pp
18. Okubo T (1988) J Chem Soc Faraday Trans 1 84:1163
19. Okubo T, Okada S, Tsuchida A (1997) J Colloid Interface Sci 189:337
20. Okubo T, Okada S (1997) J Colloid Interface Sci 192:490
21. Okubo T, Ishiki H (1999) J Colloid Interface Sci 211:151
22. Okubo T, Tsuchida A, Kato T (1999) Colloid Polymer Sci 277:191
23. (a) Okubo T, Tsuchida A, Okuda T, Fujitsuna K, Ishikawa M, Morita T, Tada T (1999) Colloids Surf A 160:311; (b) Okubo T, Tsuchida A, Okuda T, Fujitsuna K, Ishikawa M, Morita T, Tada T (1999) Colloids Surf A 153:515
24. Okubo T, Tsuchida A, Takahashi S, Taguchi K, Ishikawa M (2000) Colloid Polym Sci 278:202
25. Okubo T, Ishiki H (2000) J Colloid Interface Sci 228:151
26. Tsuchida H, Taguchi K, Takyo E, Yoshimi H, Kiriyama K, Okubo T, Ishikawa M (2000) Colloid Polym Sci 278:872
27. Okubo T, Okada S (1998) J Colloid Interface Sci 204:198
28. Yoshinaga K, Nakanishi K (1994) Composite Interfaces 2:95
29. Frenkel J (1932) Phys Z Sowjetunion 1:498
30. Hartman P (ed) (1973) Crystal growth: an introduction. North-Holland, Amsterdam
31. Okubo T (1986) J Chem Soc Faraday Trans 82:3163
32. Dhont JKG, Smits C, Lekkerkerker HNW (1992) J Colloid Interface Sci 152:386
33. Okubo T (1994) Langmuir 10:1695
34. Okubo T (1994) Langmuir 10:3529